

# PPI-SVRG: Unifying Prediction-Powered Inference and Variance Reduction for Semi-Supervised Optimization

Ruicheng Ao<sup>1</sup>, Hongyu Chen<sup>1</sup>, Haoyang Liu<sup>2</sup>, David Simchi-Levi<sup>1</sup>, and Will Wei Sun<sup>3</sup>

<sup>1</sup>Institute for Data, Systems, and Society, Massachusetts Institute of Technology, [{aorc, chenhy, dslevi}@mit.edu](mailto:{aorc, chenhy, dslevi}@mit.edu)

<sup>2</sup>Department of Mathematics, Washington University in Saint Louis, [haoyangl@wustl.edu](mailto:haoyangl@wustl.edu)

<sup>3</sup>Daniels School of Business, Purdue University, [sun244@purdue.edu](mailto:sun244@purdue.edu)

## Abstract

We study semi-supervised stochastic optimization when labeled data is scarce but predictions from pre-trained models are available. PPI and SVRG both reduce variance through control variates—PPI uses predictions, SVRG uses reference gradients. We show they are mathematically equivalent and develop PPI-SVRG, which combines both. Our convergence bound decomposes into the standard SVRG rate plus an error floor from prediction uncertainty. The rate depends only on loss geometry; predictions affect only the neighborhood size. When predictions are perfect, we recover SVRG exactly. When predictions degrade, convergence remains stable but reaches a larger neighborhood. Experiments confirm the theory: PPI-SVRG reduces MSE by 43–52% under label scarcity on mean estimation benchmarks and improves test accuracy by 2.7–2.9 percentage points on MNIST with only 10% labeled data.

**Keywords:** Prediction-Powered Inference, Stochastic Variance Reduced Gradient, Semi-supervised Learning, Variance Reduction, Control Variates, Stochastic Optimization

## 1 Introduction

A central bottleneck in machine learning and statistical inference is the cost of obtaining labeled data. Reliable estimation typically requires substantial labeled samples, yet collecting labels can be expensive, slow, or ethically constrained. At the same time, many applications provide abundant unlabeled covariates and access to externally trained models that generate cheap outcome predictions.

This data landscape—scarce labels, abundant predictions—arises across domains. In remote sensing, satellite imagery is plentiful but ground-truth labels require costly field surveys [Jean et al., 2016]. In clinical trials, patient outcomes take months to observe, yet prognostic models can predict responses from baseline characteristics [Schmidli et al., 2020, Rahman et al., 2021]. In computational biology, protein structures were historically determined through expensive crystallography, but AlphaFold now predicts structures with near-experimental accuracy [Jumper et al., 2021]. These examples share a common structure: labeled data is the bottleneck, while predictions from pre-trained models are readily available.

Prediction-Powered Inference (PPI) [Angelopoulos et al., 2023a] formalizes this setting for statistical estimation. PPI uses predictions as control variates: even imperfect predictions carry information about the target, enabling lower-variance estimators. The key insight is that predictions,

though potentially biased, are correlated with true outcomes. This correlation drives variance reduction through the classical control variate mechanism.

PPI was designed for statistical estimation—computing confidence intervals, testing hypotheses, and estimating population parameters. But many machine learning tasks require *optimization*: training models by minimizing empirical loss. Can the same control variate principle accelerate stochastic optimization?

SVRG [Johnson and Zhang, 2013] reduces variance in stochastic optimization through a complementary strategy: it uses a reference gradient computed at a snapshot point as a control variate, achieving linear convergence for strongly convex objectives. The snapshot gradient anchors the stochastic updates, reducing variance without introducing bias.

We observe that PPI and SVRG share the same mathematical structure: both subtract a correlated term and add back its expectation. PPI uses predictions; SVRG uses reference gradients. Despite their different origins—statistical estimation for PPI, optimization for SVRG—they implement the same variance reduction mechanism. This structural equivalence suggests a natural combination.

We develop PPI-SVRG, which combines both control variates to accelerate semi-supervised optimization. Our contributions are:

1. **Algorithmic framework.** We present PPI-SVRG (Algorithm 1), which computes snapshot gradients using predictions on abundant unlabeled data ( $N$  samples) rather than scarce labeled data ( $n$  samples). When  $N \gg n$ , the snapshot gradient has near-zero variance, providing a stable anchor for variance reduction.
2. **Convergence analysis.** We prove that PPI-SVRG converges at rate  $O(\alpha^s)$  for strongly convex objectives (Theorem 5.2) and  $O(1/T)$  for general convex objectives (Theorem 5.5), matching standard SVRG rates. The bounds decompose into two additive terms: an optimization term (rate  $\alpha$ , depending only on loss geometry) and a prediction-dependent error floor (the conditional variance  $\text{Var}(\nabla \ell | X, F)$ ). This separation ensures stability: poor predictions enlarge the error floor but do not slow convergence or cause divergence.
3. **Empirical validation.** Experiments on mean estimation and semi-supervised deep learning confirm the theory. PPI-SVRG reduces MSE by 43–52% under label scarcity on benchmark datasets and improves test accuracy by 2.7–2.9 percentage points on MNIST with only 10% labeled data.

How do prediction errors affect convergence? One might expect errors to slow convergence, as in noisy gradient descent. Our analysis shows a different picture: the two contributions are additive and independent. Better predictions shrink the error floor but do not speed up the rate; worse predictions enlarge the neighborhood but do not slow it down. When predictions equal true labels ( $F = Y$ ), the conditional variance vanishes and our bound reduces to the standard SVRG rate—confirming that PPI-SVRG generalizes SVRG.

## 2 Related Work

**Prediction-Powered Inference.** Prediction-powered inference (PPI) [Angelopoulos et al., 2023a,b, Zrnic and Candès, 2024b] assumes access to true labels for only a subset of data, with predictions from an external model for the remainder. PPI uses predictions as control variates to reduce variance when estimating population parameters. Extensions include active label collection [Zrnic and Candès, 2024a] and joint optimization of sampling and measurement [Ao et al., 2024]. These methods target parameter estimation—means, quantiles, regression coefficients—rather than optimization. We

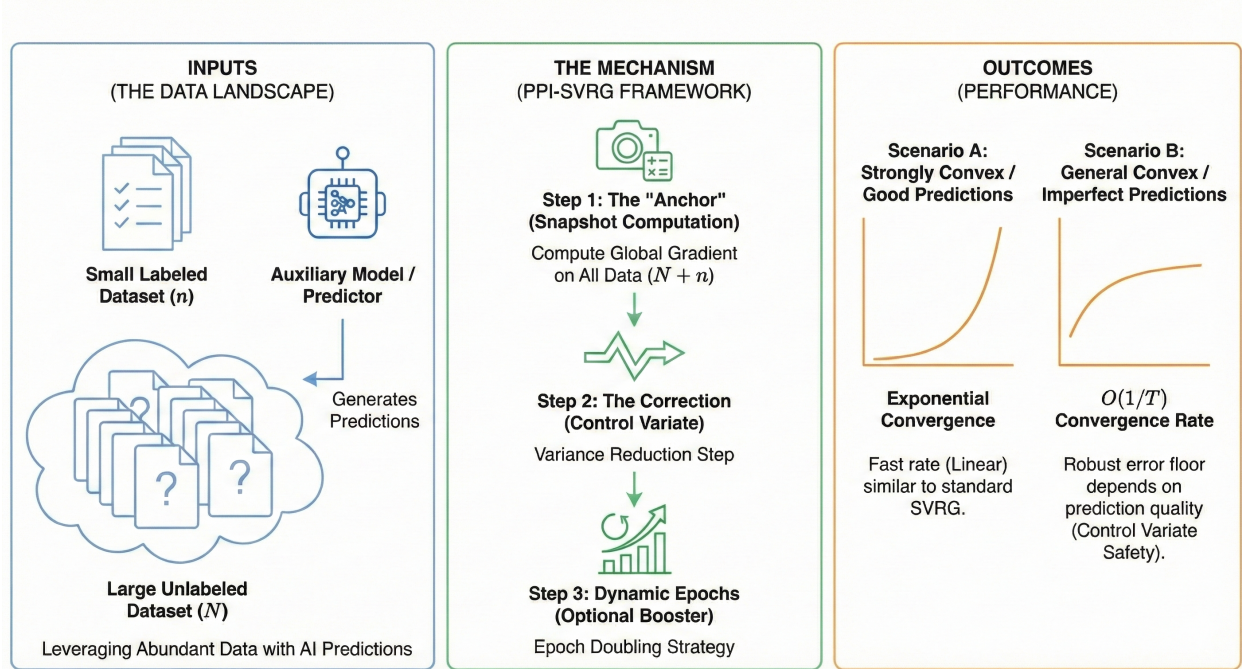


Figure 1: Overview of the PPI-SVRG framework. **Left:** The data landscape—small labeled dataset ( $n$ ) and large unlabeled dataset ( $N$ ) with predictions. **Center:** The mechanism—snapshot gradient (anchor), variance reduction (correction), and epoch doubling (booster). **Right:** Convergence outcomes—exponential for strongly convex with good predictions,  $O(1/T)$  for general convex.

Table 1: Comparison of methods. PPI-SVRG uses both control variates; the error floor  $\epsilon$  depends on prediction quality but the rate  $\alpha$  does not.

| Method          | Data    | Control Variate | Rate                     |
|-----------------|---------|-----------------|--------------------------|
| SGD             | Labeled | —               | $O(1/\sqrt{T})$          |
| SVRG            | Labeled | Reference grad. | $O(\alpha^s)$            |
| PPI             | Both    | Predictions     | (Estimation)             |
| <b>PPI-SVRG</b> | Both    | Both            | $O(\alpha^s) + \epsilon$ |

extend PPI to minimizing empirical loss, where the goal is finding optimal parameters rather than estimating fixed quantities.

**Variance Reduction in Stochastic Optimization.** SVRG [Johnson and Zhang, 2013] achieves faster convergence than SGD by using the full gradient at a reference point as a control variate, enabling linear convergence for strongly convex objectives. Related methods include SAGA [Defazio et al., 2014], which maintains per-sample gradient estimates, and SARAH [Nguyen et al., 2017], which uses stochastic recursive gradients. For nonconvex objectives, SPIDER [Fang et al., 2018] and PAGE [Li et al., 2021] achieve optimal gradient complexity. Loopless variants such as L-SVRG [Kovalev et al., 2020] eliminate the outer loop. SVRG++ [Allen-Zhu and Yuan, 2016] handles non-strongly-convex objectives via epoch doubling; we adapt this approach in PPI-SVRG++.

**Connection Between PPI and SVRG.** PPI and SVRG both use control variates, but in different contexts: PPI for estimation, SVRG for optimization. Both construct an unbiased estimator by adding and subtracting a correlated auxiliary quantity. When predictions equal labels ( $F = Y$ ),

the PPI-based gradient update reduces to the SVRG update. Section 4 develops this connection; Section 5 derives convergence bounds.

### 3 Problem Formulation

We consider loss function  $\ell_\theta(X, Y)$  with inputs  $X \in \mathcal{X}, Y \in \{-1, +1\}$ , parameterized by  $\theta \in \mathbb{R}^k$ . We seek to minimize the expected loss:

$$\min_{\theta} \quad L_\theta = \mathbb{E} [\ell_\theta(X, Y)]. \quad (1)$$

Given samples  $\{(X^i, Y^i)\}_{i=1}^n$ , the empirical loss is

$$\min_{\theta} \quad L_\theta^n = \frac{1}{n} \sum_{i=1}^n \ell_\theta(X^i, Y^i). \quad (2)$$

In many applications, labels are expensive but predictions from pre-trained models are cheap. When predictions  $F$  are available for unlabeled data, we can augment the objective to reduce variance. Let  $F(X) \in \{-1, +1\}$  denote a predictor. The augmented objective is:

$$\begin{aligned} \min_{\theta} \quad & \frac{1}{n} \sum_{i=1}^n \ell_\theta(X^i, Y^i) \\ & + \left( \frac{1}{N+n} \sum_{i=1}^{N+n} g_\theta(X^i, F^i) \right. \\ & \left. - \frac{1}{n} \sum_{i=1}^n g_\theta(X^i, F^i) \right), \end{aligned} \quad (3)$$

where  $g_\theta$  is an auxiliary function and  $F^i = F(X^i)$  denotes the prediction for sample  $i$ . We only need labels for  $n$  samples; the remaining  $N$  samples require only predictions.

The simplest choice for the auxiliary function is  $g = \ell$ . A refined choice sets  $g$  to satisfy

$$\nabla_{\theta} g_\theta(X, F) = \mathbb{E} [\nabla_{\theta} \ell_\theta(X, Y) | X, F], \quad (4)$$

where the expectation is over label  $Y$  conditional on input  $X$  and prediction  $F$ . This choice achieves semi-parametric asymptotic optimality as  $n, N \rightarrow \infty$ .

## 4 Algorithms

### 4.1 The Connection Between SVRG and PPI

PPI and SVRG both achieve variance reduction through control variates. We first review SVRG, then show how PPI shares its structure.

The stochastic variance-reduced gradient descent method (SVRG) [Johnson and Zhang, 2013] considers optimizing the empirical loss (2). It uses a double-loop strategy with  $m$  inner steps. Let  $\tilde{\theta}_s$  denote the parameter at outer loop  $s$ , and let

$$\tilde{\mu}_s = \frac{1}{n} \sum_{i=1}^n \nabla_{\theta} \ell_{\tilde{\theta}_s}(X^i, Y^i)$$

be the full gradient at  $\tilde{\theta}_s$ . The inner loop starts with  $\theta_0 = \tilde{\theta}_s$  and, for  $t = 1, \dots, m-1$ , randomly picks  $i_t \in \{1, \dots, n\}$  and updates:

$$\begin{aligned}\theta_t &= \theta_{t-1} - \eta \left( \nabla_{\theta} \ell_{\theta_{t-1}}(X^{i_t}, Y^{i_t}) \right. \\ &\quad \left. - \nabla_{\theta} \ell_{\tilde{\theta}_s}(X^{i_t}, Y^{i_t}) + \tilde{\mu}_s \right).\end{aligned}\tag{5}$$

The outer loop then sets  $\tilde{\theta}_{s+1} = \theta_t$  for a randomly chosen  $t \in \{0, \dots, m-1\}$ .

Under the standard smoothness and strong convexity assumptions:

$$\begin{aligned}\ell_{\theta}(X^i, Y^i) - \ell_{\theta'}(X^i, Y^i) &\leq \langle \nabla_{\theta'}, \theta - \theta' \rangle + 0.5\lambda \|\theta - \theta'\|_2,\end{aligned}\tag{6}$$

$$\begin{aligned}L_{\theta}^n - L_{\theta'}^n &\geq \langle \nabla_{\theta} L_{\theta'}^n, \theta - \theta' \rangle + 0.5\gamma \|\theta - \theta'\|_2^2.\end{aligned}\tag{7}$$

SVRG achieves exponential convergence with rate  $\alpha = 1/[\gamma\eta(1 - 2\lambda\eta)m] + 2\lambda\eta/(1 - 2\lambda\eta) < 1$  [Johnson and Zhang, 2013].

Prediction-Powered Inference [Angelopoulos et al., 2023a] augments the empirical loss with a correction term using predictions on unlabeled data. Recall the PPI objective (3):

$$\begin{aligned}\min_{\theta} \frac{1}{n} \sum_{i=1}^n \ell_{\theta}(X^i, Y^i) &+ \left( \frac{1}{N+n} \sum_{j=1}^{N+n} g_{\theta}(X^j, F^j) \right. \\ &\quad \left. - \frac{1}{n} \sum_{i=1}^n g_{\theta}(X^i, F^i) \right).\end{aligned}$$

The auxiliary function  $g_{\theta}(X, F)$  satisfies the moment condition (4):  $\nabla_{\theta} g_{\theta}(X, F) = \mathbb{E}[\nabla_{\theta} \ell_{\theta}(X, Y) | X, F]$ . This ensures that  $\nabla_{\theta} g_{\theta}$  is an unbiased proxy for the true gradient, enabling variance reduction through the control variate mechanism.

The gradient of the PPI objective decomposes as:

$$\begin{aligned}\nabla_{\theta} L_{\theta}^{\text{PPI}} &= \frac{1}{n} \sum_{i=1}^n \nabla_{\theta} \ell_{\theta}(X^i, Y^i) \\ &+ \left( \frac{1}{N+n} \sum_{j=1}^{N+n} \nabla_{\theta} g_{\theta}(X^j, F^j) \right. \\ &\quad \left. - \frac{1}{n} \sum_{i=1}^n \nabla_{\theta} g_{\theta}(X^i, F^i) \right).\end{aligned}$$

When  $N \gg n$ , the second term has low variance—it is computed on abundant unlabeled data—and serves as a control variate for the stochastic gradient.

Consider the PPI-augmented loss (3) with auxiliary function  $g_{\theta}(X, F)$ . Define the augmented gradient as

$$\tilde{\mu}_s = \mathbb{E} \left[ \nabla_{\theta} g_{\tilde{\theta}_s}(X, F) \right],\tag{8}$$

---

**Algorithm 1** PPI-SVRG (Strongly Convex)

---

**Input:** Initial parameter  $\tilde{\theta}_0$ , step size  $\eta$ , epochs  $S$ , inner steps  $m$

**Output:** Optimized parameter  $\tilde{\theta}_S$

**for**  $s = 0$  to  $S - 1$  **do**

    Compute  $\tilde{\mu}_s = \frac{1}{N+n} \sum_{j=1}^{N+n} \nabla_{\theta} g_{\tilde{\theta}_s}(X^j, F^j)$

    Initialize:  $\theta_0 = \tilde{\theta}_s$

**for**  $t = 0$  to  $m - 1$  **do**

        Sample  $i_t \sim \text{Uniform}(\{1, \dots, n\})$

        Update  $\theta_{t+1}$  via (9)

**end for**

    Sample  $\tau \sim \text{Uniform}(\{0, \dots, m - 1\})$

    Set  $\tilde{\theta}_{s+1} = \theta_{\tau}$

**end for**

---

which can be estimated using the unlabeled data. The PPI-based update is:

$$\begin{aligned} \theta_t = \theta_{t-1} - \eta & \left( \nabla_{\theta} \ell_{\theta_{t-1}}(X^{i_t}, Y^{i_t}) \right. \\ & \left. - \nabla_{\theta} g_{\tilde{\theta}_s}(X^{i_t}, F^{i_t}) + \tilde{\mu}_s \right). \end{aligned} \quad (9)$$

When  $g = \ell$  and  $F = Y$ , the PPI update (9) has the same structure as the SVRG update (5). The term  $\nabla_{\theta} g_{\tilde{\theta}_s}(X^{i_t}, F^{i_t})$  becomes  $\nabla_{\theta} \ell_{\tilde{\theta}_s}(X^{i_t}, Y^{i_t})$ , matching SVRG, and the augmented gradient  $\tilde{\mu}_s = \mathbb{E}[\nabla_{\theta} \ell_{\tilde{\theta}_s}(X, Y)]$  equals the full gradient used in SVRG (in the population sense).

The difference lies in the snapshot gradient  $\tilde{\mu}_s$ : SVRG uses the empirical average over  $n$  labeled samples, while PPI uses the expectation estimated from  $N + n$  samples with predictions.

Both updates have identical structure: subtract a correlated term and add back its expectation. When  $F = Y$ , the variance term in our convergence bound vanishes, recovering the SVRG rate. When  $F \neq Y$ , the control variate  $\nabla_{\theta} g_{\tilde{\theta}_s}(X, F)$  uses predictions instead of true labels. Large unlabeled datasets reduce variance, and the convergence bound includes an additional term quantifying prediction uncertainty.

Algorithm 1 presents PPI-SVRG, which maintains SVRG's double-loop structure but computes the snapshot gradient over both labeled and unlabeled data.

The key difference from standard SVRG is Line 5: the snapshot gradient  $\tilde{\mu}_s$  uses all  $N + n$  samples, not just the  $n$  labeled samples. The inner loop (Lines 7–9) samples a labeled point at each iteration and applies update (9), using predictions  $F^{i_t}$  in the control variate. Lines 10–11 randomly select one inner iterate as the next snapshot, following standard SVRG.

When  $F = Y$ , Algorithm 1 reduces to standard SVRG.

**Intuition: Why does the control variate help?** The update (9) can be rewritten as:

$$\theta_t = \theta_{t-1} - \eta \left[ \underbrace{\nabla \ell_{\theta_{t-1}}(X^{i_t}, Y^{i_t}) - \nabla g_{\tilde{\theta}_s}(X^{i_t}, F^{i_t})}_{\text{residual}} + \underbrace{\tilde{\mu}_s}_{\text{anchor}} \right].$$

The residual term  $\nabla \ell - \nabla g$  has lower variance than  $\nabla \ell$  alone when  $\nabla g$  is correlated with  $\nabla \ell$ —this is the essence of control variates. Adding back the anchor  $\tilde{\mu}_s$  ensures the update direction is unbiased. When  $F$  is informative about  $Y$ , the conditional expectation  $\nabla g = \mathbb{E}[\nabla \ell | X, F]$  closely tracks the true

---

**Algorithm 2** PPI-SVRG++ (General Convex with Epoch Doubling)

---

**Input:** Initial parameter  $\tilde{\theta}_0$ , step size  $\eta$ , epochs  $S$ , initial inner steps  $m_0$

**Output:** Optimized parameter  $\tilde{\theta}_S$

Initialize:  $\theta_0^1 = \tilde{\theta}_0$

**for**  $s = 1$  to  $S$  **do**

    Set epoch length:  $m_s = m_0 \cdot 2^{s-1}$

    Compute  $\tilde{\mu}_{s-1} = \frac{1}{N+n} \sum_{j=1}^{N+n} \nabla_{\theta} g_{\tilde{\theta}_{s-1}}(X^j, F^j)$

**for**  $t = 0$  to  $m_s - 1$  **do**

        Sample  $i_t \sim \text{Uniform}(\{1, \dots, n\})$

        Update  $\theta_{t+1}^s$  via (10)

**end for**

    Set snapshot:  $\tilde{\theta}_s = \frac{1}{m_s} \sum_{t=0}^{m_s-1} \theta_t^s$

    Set next start:  $\theta_0^{s+1} = \theta_{m_s}^s$

**end for**

---

gradient, and the residual captures only the unpredictable component. The variance reduction is greatest when predictions are accurate and abundant unlabeled data makes  $\tilde{\mu}_s$  nearly deterministic.

## 4.2 PPI-SVRG++ for General Convex Objectives

PPI-SVRG++ extends PPI-SVRG to general convex objectives (without strong convexity), adapting the SVRG++ framework [Allen-Zhu and Yuan, 2016].

The key idea is epoch doubling: instead of a fixed inner loop length  $m$ , the number of inner iterations  $m_s$  doubles each epoch. In strongly convex settings, fixed epoch length suffices for exponential convergence. Without strong convexity, we must balance early exploration (short epochs) with final refinement (long epochs). Setting  $m_s = m_0 \cdot 2^{s-1}$  achieves  $O(1/T)$  convergence, matching the optimal rate for general convex optimization.

Let  $m_0$  be the initial inner loop length. For each outer loop  $s = 1, \dots, S$ , the algorithm proceeds as follows. The epoch length is set to  $m_s = m_0 \cdot 2^{s-1}$ , doubling each epoch. The snapshot gradient is computed on all samples:

$$\tilde{\mu}_{s-1} = \frac{1}{N+n} \sum_{j=1}^{N+n} \nabla_{\theta} g_{\tilde{\theta}_{s-1}}(X^j, F^j).$$

The inner loop initializes  $\theta_0^s = \theta_{m_{s-1}}^{s-1}$  (continuing from the previous epoch's last iterate, with  $\theta_0^1 = \tilde{\theta}_0$ ) and updates for  $t = 0, \dots, m_s - 1$ :

$$\begin{aligned} \theta_{t+1}^s &= \theta_t^s - \eta \left( \nabla_{\theta} \ell_{\theta_t^s}(X^{i_t}, Y^{i_t}) \right. \\ &\quad \left. - \nabla_{\theta} g_{\tilde{\theta}_{s-1}}(X^{i_t}, F^{i_t}) + \tilde{\mu}_{s-1} \right). \end{aligned} \quad (10)$$

The snapshot is updated by averaging:  $\tilde{\theta}_s = \frac{1}{m_s} \sum_{t=0}^{m_s-1} \theta_t^s$ , ensuring optimal variance reduction as in standard SVRG++. The next epoch then starts from the last iterate:  $\theta_0^{s+1} = \theta_{m_s}^s$ .

With this modification, PPI-SVRG++ achieves fast convergence rates even when the objective is not strongly convex (e.g., Lasso-PPI). Algorithm 2 presents the complete PPI-SVRG++ with epoch doubling.

Algorithm 2 extends Algorithm 1 in three ways. First, the epoch length doubles each epoch (Line 6). Second, the inner loop continues from the previous epoch’s last iterate rather than restarting from the snapshot. Third, the snapshot is the average of all inner iterates (Line 12), not a random selection.

These modifications enable  $O(1/T)$  convergence without strong convexity, whereas Algorithm 1 requires strong convexity for exponential convergence.

## 5 Theoretical Analysis

### 5.1 Convergence under Strong Convexity

We analyze the convergence of Algorithm 1 under strong convexity. The bound decomposes into the standard SVRG rate plus a term capturing prediction uncertainty.

**Assumption 5.1** (Smoothness and Strong Convexity). Each component loss  $\ell_\theta(X^i, Y^i)$  is  $\lambda$ -smooth (6), and the empirical loss  $L_\theta^n$  is  $\gamma$ -strongly convex (7).

When  $g = \theta^\top \mathbb{E}[\ell|X, F]$ , we have the following result.

**Theorem 5.2** (Convergence of PPI-SVRG). *Under Theorem 5.1, for  $s \geq 1$ , we have*

$$\begin{aligned} & \mathbb{E}[L_{\theta_s}^n - L_{\theta_*}^n] \\ & \leq \underbrace{\alpha^s \mathbb{E}[L_{\theta_0}^n - L_{\theta_*}^n]}_{\text{SVRG term}} \\ & \quad + \underbrace{\beta \frac{1 - \alpha^s}{1 - \alpha} \mathbb{E}[\text{Var}(\nabla_\theta \ell_{\theta_*}(X^i, Y^i) | X^i, F^i)]}_{\text{pred. uncertainty}} \end{aligned} \quad (11)$$

where  $\alpha = 1/[\gamma\eta(1 - 2\lambda\eta)m] + 2\lambda\eta/(1 - 2\lambda\eta) < 1$  and  $\beta = \eta/(1 - 2\lambda\eta)$ .

The first term,  $\alpha^s \mathbb{E}[L_{\theta_0}^n - L_{\theta_*}^n]$ , is the standard SVRG rate—exponential decay with  $\alpha < 1$ , identical to Johnson and Zhang [2013]. The second term captures prediction uncertainty:  $\text{Var}(\nabla_\theta \ell_{\theta_*}(X, Y) | X, F)$  measures the gradient information that remains hidden after observing the prediction  $F$ .

When  $F = Y$ , the conditional variance vanishes because  $Y$  is determined by  $(X, F)$ :

$$\text{Var}(\nabla_\theta \ell_{\theta_*}(X, Y) | X, F = Y) = 0.$$

The bound (11) then reduces to the standard SVRG bound:

$$\mathbb{E}[L_{\theta_s}^n - L_{\theta_*}^n] \leq \alpha^s \mathbb{E}[L_{\theta_0}^n - L_{\theta_*}^n].$$

This confirms that PPI and SVRG share the same control variate structure.

The bound interpolates between two extremes. Perfect predictions ( $F = Y$ ) recover the SVRG rate. Imperfect predictions cause convergence to a neighborhood whose size depends on prediction quality—better predictions shrink this neighborhood, but the exponential rate  $\alpha$  remains unchanged. The two contributions are additive and independent:  $\alpha$  depends only on loss geometry  $(\lambda, \gamma, \eta, m)$ , while the error floor depends only on how informative  $F$  is about  $Y$ . This separation ensures stability—the algorithm never diverges due to poor predictions; it simply converges to a larger neighborhood.

*Remark 5.3* (Extreme Cases). When  $F$  is independent of  $Y$  given  $X$ , the conditional variance  $\text{Var}(\nabla\ell|X, F)$  equals the marginal variance  $\text{Var}(\nabla\ell|X)$ —predictions provide no information, and PPI-SVRG reduces to standard SVRG on labeled data. When  $F = Y$ , the conditional variance vanishes and we recover the exact SVRG rate. Between these extremes, the error floor interpolates smoothly according to prediction quality.

*Remark 5.4* (When is PPI-SVRG Most Useful?). The bound suggests PPI-SVRG is most beneficial when: (i) labeled data is scarce ( $n$  small), so the baseline has high variance; (ii) unlabeled data is abundant ( $N \gg n$ ), so the snapshot gradient  $\tilde{\mu}_s$  has low variance; and (iii) predictions are informative ( $\text{Var}(\nabla\ell|X, F) \ll \text{Var}(\nabla\ell|X)$ ), so the error floor is small. In contrast, when labeled data is abundant or predictions are uninformative, PPI-SVRG offers little advantage over standard SVRG.

The auxiliary function  $g_\theta(X, F) = \mathbb{E}[\ell_\theta(X, Y) \mid X, F]$  makes  $\ell_\theta - g_\theta$  have zero conditional mean given  $(X, F)$ . This allows the law of total variance to decompose the gradient variance into optimization and prediction components. The residual variance is exactly  $\text{Var}(\nabla\ell_\theta|X, F)$ —the gradient uncertainty that remains after observing the prediction.

*Proof sketch.* Decompose the variance of the update direction  $v_t$  into two components: one depending on distance to the optimum (as in SVRG), one capturing prediction uncertainty. The first is bounded via smoothness, following standard SVRG analysis. For the second, since  $\nabla_\theta g_\theta(X, F) = \mathbb{E}[\nabla_\theta \ell_\theta(X, Y)|X, F]$ , the residual variance equals the conditional variance given predictions. Summing over iterations and applying the total variance formula yields the bound. See Section A for details.

## 5.2 Convergence under General Convexity

We extend the analysis to general convex objectives using Algorithm 2.

**Theorem 5.5** (Convergence of PPI-SVRG++). *Assume  $\ell_\theta$  and  $g_\theta$  are convex and  $\lambda$ -smooth. Let  $T = \sum_{s=1}^S m_s$  be the total number of inner iterations. With epoch lengths  $m_s = m_0 \cdot 2^{s-1}$  and step size  $\eta < 1/(4\lambda)$ , PPI-SVRG++ satisfies:*

$$\begin{aligned} \mathbb{E}[L_{\tilde{\theta}_S}^n - L_{\theta_*}^n] &\leq O\left(\frac{\|\theta_0 - \theta_*\|^2}{\eta T}\right) \\ &\quad + C(\eta\sigma_{PPI}^2 + D\epsilon_{bias}), \end{aligned} \tag{12}$$

where  $\sigma_{PPI}^2 = \max_\theta \mathbb{E}[\|\nabla\ell(\theta) - \nabla g(\theta)\|^2]$  is the irreducible variance of the control variate, and  $\epsilon_{bias} = \|\nabla \hat{L}_{N+n}^g - \nabla \hat{L}_n^g\|$  is the PPI estimation bias.

Note that  $\sigma_{PPI}^2 = \max_\theta \text{Var}(\nabla\ell_\theta|X, F)$ , since  $\nabla g = \mathbb{E}[\nabla\ell|X, F]$ . This upper bounds the variance at the optimum appearing in Theorem 5.2.

PPI-SVRG++ converges at  $O(1/T)$  to a prediction-dependent error floor, matching the optimal rate for smooth convex optimization. The error floor  $O(\eta\sigma_{PPI}^2)$  shrinks with more accurate predictors (smaller  $\sigma_{PPI}$ ) or larger unlabeled datasets (smaller  $\epsilon_{bias}$ ).

*Remark 5.6* (Comparison with Standard SVRG). Standard SVRG computes the snapshot gradient using  $n$  labeled samples. PPI-SVRG++ uses  $N + n$  samples (with predictions on the unlabeled portion), reducing the snapshot gradient variance when  $N \gg n$ . The convergence rate remains  $O(1/T)$ , matching the optimal rate for smooth convex optimization. The cost is a prediction-dependent error floor that shrinks as predictions improve.

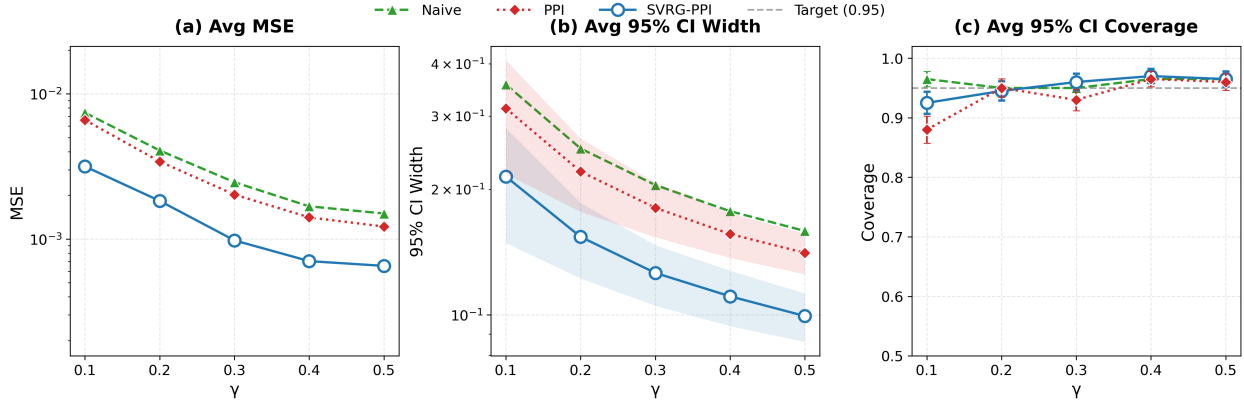


Figure 2: Mean estimation on `forest`: MSE, CI width, and coverage across labeled proportions  $\gamma$ . PPI-SVRG achieves the lowest MSE and narrowest CIs while maintaining valid coverage. Lower is better for MSE and CI width; 95% is nominal for coverage.

## 6 Experiments

We evaluate PPI-SVRG on two tasks: mean estimation under label scarcity, and deep learning with limited supervision. PPI-SVRG reduces MSE by 43–52% under label scarcity ( $\gamma = 0.1$ ) on the mean estimation tasks and improves test accuracy by 2.7–2.9 % on MNIST.

### 6.1 Mean Estimation

We consider estimating the population mean  $\theta_* = \mathbb{E}[Y]$  using a small labeled set and a large pool of predictions. We compare three methods: Naive (labeled data only), PPI, and PPI-SVRG (Algorithm 1).

We use two datasets from the PPI benchmark [Angelopoulos et al., 2023a]: `forest` for deforestation in the Amazon Rainforest ( $n = 160$  labeled,  $N = 1,436$  unlabeled), and `galaxies` for galaxy morphology classification ( $n = 1,674$  labeled,  $N = 15,069$  unlabeled). We obtain calibrated predictions via CatBoost [Prokhorenkova et al., 2018] with 5-fold cross-fitting to ensure predictor independence from labeled samples (details in Appendix C.1). For each labeled proportion  $\gamma \in \{0.1, 0.2, 0.3, 0.4, 0.5\}$ , we perform 200 Monte Carlo repetitions and report MSE, 95% CI width, and coverage probability.

Figures 2 and 3 show that PPI-SVRG achieves lower MSE and narrower confidence intervals than both Naive and PPI, while maintaining valid coverage. The gains are largest under label scarcity: at  $\gamma = 0.1$ , PPI-SVRG reduces MSE by 52.1% (forest) and 43.4% (galaxies) relative to PPI. This aligns with Theorem 5.2: the convergence bound depends on the conditional variance  $\mathbb{E}[\text{Var}(\nabla_\theta \ell_{\theta_*} | X, F)]$ , which calibrated predictions reduce.

Some patterns stand out. First, the relative improvement *decreases* as  $\gamma$  increases: at  $\gamma = 0.5$ , MSE reduction drops to 46.41% (forest) and 19.98% (galaxies). This is expected as abundant labeled data already yields low-variance baselines, leaving less room for improvement. Second, PPI-SVRG exhibits relatively high coverage probability across both datasets with greater stability than PPI, and stays closest to the nominal 95% level on `galaxies`. Naive tends to over-cover on `forest` but under-covers on `galaxies`; PPI occasionally under-covers at small  $\gamma$ .

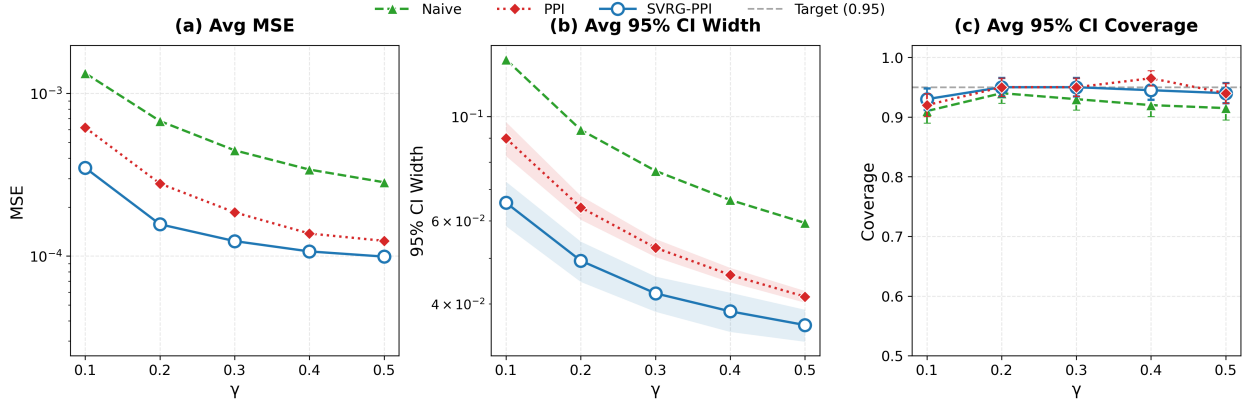


Figure 3: Mean estimation on galaxies: PPI-SVRG achieves consistent improvements, with coverage closest to the nominal 95%.

## 6.2 Semi-Supervised Deep Learning

We apply PPI-SVRG to semi-supervised image classification on MNIST using DeepOBS benchmark suite [Schneider et al., 2019]. Note that PPI is not included as a baseline: PPI targets statistical estimation (e.g., computing population means or confidence intervals), not optimization. Standard SVRG, conversely, is an optimization algorithm that cannot leverage unlabeled data. PPI-SVRG bridges this gap—it applies variance reduction to optimization while using predictions on unlabeled data.

We split the 60K MNIST training set into two parts: 30K for training a predictor (2C2D architecture, 99.16% test accuracy), and 30K for the main experiment, of which only 10% (3K) have labels. The student model is an MLP. We compare Baseline (Adam/Momentum) against PPI-SVRG variants using the same optimizer. All methods train for 50 epochs with batch size 256 over 5 random seeds (implementation details in Appendix C.2).

Figure 4 shows validation and test metrics across training. PPI-SVRG initially underperforms (weak correlation between snapshot and current parameters) but surpasses baselines as training progresses and variance reduction takes effect. The learning curves reveal three phases. In the *warm-up phase*, PPI-SVRG trails baselines. The snapshot gradient  $\tilde{\mu}_s$  is computed at the previous epoch’s parameters, which poorly approximate the current gradient when parameters change rapidly. The ramp-up coefficient  $\lambda_u(t)$  (Appendix C.2) mitigates this by down-weighting the control variate early on. In the *transition phase*, the gap narrows as parameters stabilize. The snapshot becomes a better anchor. In the *steady-state phase*, PPI-SVRG dominates. Variance reduction takes over, and the large unlabeled dataset ( $N = 27K$  vs.  $n = 3K$ ) provides a nearly deterministic snapshot gradient.

Table 2 reports final test accuracy with 95% confidence intervals. PPI-SVRG-Momentum improves over Baseline-Momentum by +2.69 %; PPI-SVRG-Adam improves over Baseline-Adam by +2.94 %. These gains are consistent across seeds and orthogonal to the choice of optimizer, confirming that the benefit stems from improved gradient estimation rather than optimizer-specific effects.

The strong predictor ( $F$  with 99.16% accuracy) ensures that  $\nabla_\theta g_\theta(X, F) \approx \mathbb{E}[\nabla_\theta \ell_\theta(X, Y) \mid X, F]$ , enabling effective variance reduction. As  $N \gg n$ , the snapshot gradient  $\tilde{\mu}_s$  has low variance, providing a stable anchor for the control variate correction.

These results validate Theorem 5.2. First, the *rate* is preserved: PPI-SVRG and baselines both

**Learning Curves (Mean  $\pm$  Std over Seeds)**  
**Aligned by Training Iteration**

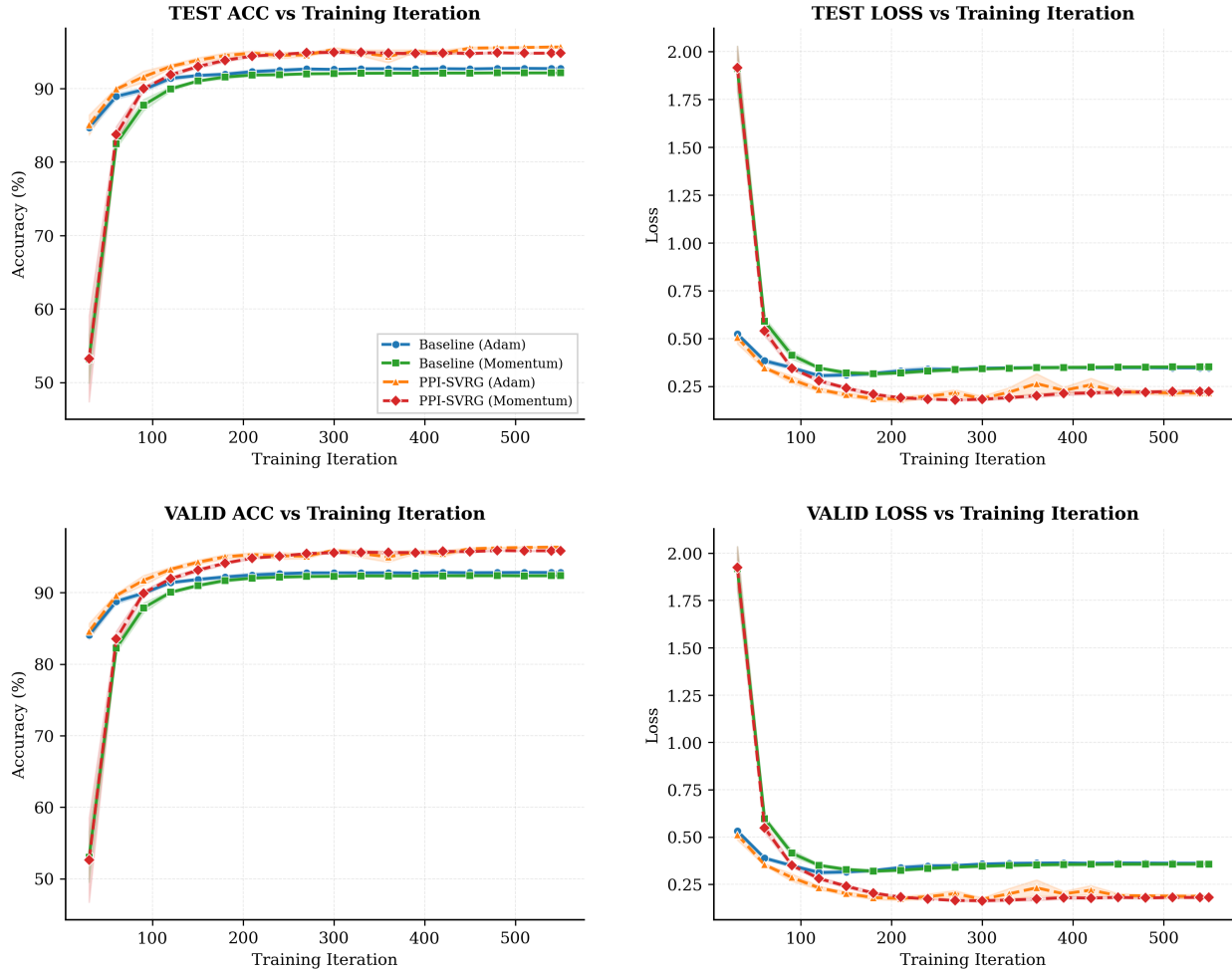


Figure 4: Learning curves on MNIST (mean  $\pm$  std over 5 seeds). PPI-SVRG variants achieve higher accuracy and lower loss than baselines after an initial warm-up phase.

reach near-final performance by around 200 iterations, but PPI-SVRG converges to a better solution. This matches the theorem— $\alpha$  is independent of prediction quality. Second, the *error floor* shrinks with better predictions: the near-perfect predictor (99.16% accuracy) yields small  $\text{Var}(\nabla \ell | X, F)$ , explaining the +2.7–2.9 pp gains. Third, the algorithm remains stable even when the control variate is misaligned (warm-up phase): the additive structure of the bound ensures PPI-SVRG does not diverge but simply converges more slowly. For practitioners, two guidelines emerge: PPI-SVRG benefits most from large unlabeled datasets ( $N \gg n$ ) and accurate predictors; and patience is required during warm-up while early stopping at beginning stage would incorrectly favor baselines.

## 7 Conclusion

PPI and SVRG both reduce variance through control variates. We combined them into PPI-SVRG, with convergence bounds that decompose into optimization error and prediction error. The rate  $\alpha$

Table 2: Test accuracy with 95% CI over 5 seeds.

| Method            | Accuracy [95% CI]     |
|-------------------|-----------------------|
| Baseline-Adam     | 92.70% [92.60, 92.81] |
| Baseline-Momentum | 92.12% [92.11, 92.14] |
| PPI-SVRG-Adam     | 95.64% [95.51, 95.77] |
| PPI-SVRG-Momentum | 94.81% [94.68, 94.94] |

depends on loss geometry; predictions affect only the neighborhood size. Poor predictions enlarge the neighborhood but do not cause instability. Experiments confirm this: PPI-SVRG reduces MSE by 43–52% under label scarcity ( $\gamma = 0.1$ ) on the forest and galaxies datasets, and improves test accuracy by 2.7–2.9 percentage points on MNIST.

The experiments show three patterns. First, improvements are largest under label scarcity: at 10% labeled data, PPI-SVRG achieves over 50% MSE reduction, while the gap narrows at higher labeled proportions. Second, the method requires a warm-up phase in deep learning: PPI-SVRG initially underperforms baselines (epochs 1–10) before surpassing them once parameters stabilize. Third, predictor quality matters: higher-correlation predictors yield larger gains, as reflected in the conditional variance term of Theorem 5.2.

Two limitations: (i) PPI-SVRG requires predictions on unlabeled data, so its benefits diminish when predictions are unavailable or poorly calibrated; (ii) highly inaccurate predictors provide limited variance reduction, though the algorithm remains stable.

Future work could extend PPI-SVRG to non-convex objectives, develop adaptive step size and epoch length selection, explore combinations with SAGA or momentum-based methods, and investigate automatic warm-up scheduling based on snapshot-parameter correlation.

## References

Kingma DP Ba J Adam et al. A method for stochastic optimization. *arXiv preprint arXiv:1412.6980*, 1412(6), 2014.

Zeyuan Allen-Zhu and Yang Yuan. Improved svrg for non-strongly-convex or sum-of-non-convex objectives. In Maria Florina Balcan and Kilian Q. Weinberger, editors, *Proceedings of The 33rd International Conference on Machine Learning*, volume 48 of *Proceedings of Machine Learning Research*, pages 1080–1089, New York, New York, USA, 20–22 Jun 2016. PMLR. URL <https://proceedings.mlr.press/v48/allen-zhub16.html>.

Anastasios N Angelopoulos, Stephen Bates, Clara Fannjiang, Michael I Jordan, and Tijana Zrnic. Prediction-powered inference. *Science*, 382(6671):669–674, 2023a.

Anastasios N Angelopoulos, John C Duchi, and Tijana Zrnic. Ppi++: Efficient prediction-powered inference. *arXiv preprint arXiv:2311.01453*, 2023b.

Ruicheng Ao, Hongyu Chen, and David Simchi-Levi. Prediction-guided active experiments. *arXiv preprint*, 2024.

Sébastien Bubeck. Convex optimization: Algorithms and complexity. *Foundations and Trends in Machine Learning*, 8(3-4):231–357, 2015.

Aaron Defazio, Francis Bach, and Simon Lacoste-Julien. Saga: A fast incremental gradient method with support for non-strongly convex composite objectives. In *Advances in Neural Information Processing Systems*, pages 1646–1654, 2014.

Cong Fang, Chris Junchi Li, Zhouchen Lin, and Tong Zhang. Spider: Near-optimal non-convex optimization via stochastic path-integrated differential estimator. In *Advances in Neural Information Processing Systems*, pages 687–697, 2018.

Neal Jean, Marshall Burke, Michael Xie, W Matthew Davis, David B Lobell, and Stefano Ermon. Combining satellite imagery and machine learning to predict poverty. *Science*, 353(6301):790–794, 2016.

Rie Johnson and Tong Zhang. Accelerating stochastic gradient descent using predictive variance reduction. *Advances in neural information processing systems*, 26, 2013.

John Jumper, Richard Evans, Alexander Pritzel, Tim Green, Michael Figurnov, Olaf Ronneberger, Kathryn Tunyasuvunakool, Russ Bates, Augustin Žídek, Anna Potapenko, et al. Highly accurate protein structure prediction with alphafold. *nature*, 596(7873):583–589, 2021.

Dmitry Kovalev, Samuel Horváth, and Peter Richtárik. Don’t jump through hoops and remove those loops: Svrg and katyusha are better without the outer loop. In *Proceedings of the 31st International Conference on Algorithmic Learning Theory*, 2020.

Zhize Li, Hongyan Bao, Xiangliang Zhang, and Peter Richtárik. Page: A simple and optimal probabilistic gradient estimator for nonconvex optimization, 2021.

Lam M Nguyen, Jie Liu, Katya Scheinberg, and Martin Takáč. Sarah: A novel method for machine learning problems using stochastic recursive gradient. In *Proc. International Conference on Machine Learning*, pages 2613–2621, 2017.

Liudmila Prokhorenkova, Gleb Gusev, Aleksandr Vorobev, Anna Veronika Dorogush, and Andrey Gulin. Catboost: unbiased boosting with categorical features. *Advances in neural information processing systems*, 31, 2018.

Rifaquat Rahman, Steffen Venzl, Jon McDunn, Bill Louv, Irmarie Reyes-Rivera, Mei-Yin C Polley, Fahar Merchant, Lauren E Abrey, Joshua E Allen, Laura K Aguilar, et al. Leveraging external data in the design and analysis of clinical trials in neuro-oncology. *The Lancet Oncology*, 22(10):e456–e465, 2021.

Heinz Schmidli, Dieter A Häring, Marius Thomas, Adrian Cassidy, Sebastian Weber, and Frank Bretz. Beyond randomized clinical trials: use of external controls. *Clinical Pharmacology & Therapeutics*, 107(4):806–816, 2020.

Frank Schneider, Lukas Balles, and Philipp Hennig. Deepobs: A deep learning optimizer benchmark suite. *arXiv preprint arXiv:1903.05499*, 2019.

Ilya Sutskever, James Martens, George Dahl, and Geoffrey Hinton. On the importance of initialization and momentum in deep learning. In *International conference on machine learning*, pages 1139–1147. pmlr, 2013.

Tijana Zrnic and Emmanuel J Candès. Active statistical inference. *arXiv preprint arXiv:2403.03208*, 2024a.

Tijana Zrnic and Emmanuel J Candès. Cross-prediction-powered inference. *Proceedings of the National Academy of Sciences*, 121(15):e2322083121, 2024b.

## A Proof of Theorem 5.2 (PPI-SVRG)

*Proof.* Given any  $i$  and  $\theta$ , we define the first-order optimality gap as

$$h_\theta^i = \ell_\theta(X^i, Y^i) - \ell_{\theta_*}(X^i, Y^i) - \langle \nabla_\theta \ell_{\theta_*}(X^i, Y^i), \theta - \theta_* \rangle.$$

It follows that  $h_{\theta_*}^i = \min_\theta h_\theta^i$  and

$$\begin{aligned} 0 &= h_{\theta_*}^i \leq \min_\eta h_{\theta - \eta \nabla_\theta h_\theta^i}^i \\ &\leq \min_\eta \left[ h_\theta^i - \eta \|\nabla_\theta h_\theta^i\|_2^2 \right. \\ &\quad \left. + 0.5\lambda\eta^2 \|\nabla_\theta h_\theta^i\|_2^2 \right] \\ &= h_\theta^i - \frac{1}{2L} \|\nabla_\theta h_\theta^i\|_2^2. \end{aligned}$$

Therefore, we have

$$\begin{aligned} &\|\nabla_\theta \ell_\theta(X^i, Y^i) - \nabla_\theta \ell_{\theta_*}(X^i, Y^i)\|_2^2 \\ &\leq 2\lambda \left[ \ell_\theta(X^i, Y^i) - \ell_{\theta_*}(X^i, Y^i) \right. \\ &\quad \left. - \langle \nabla_\theta \ell_{\theta_*}(X^i, Y^i), \theta - \theta_* \rangle \right]. \end{aligned}$$

Summing the above inequality over  $i = 1, \dots, n$  and using the fact that  $\nabla_\theta L_{\theta_*}^n = 0$ , we get

$$\frac{1}{n} \sum_{i=1}^n \|\nabla_\theta \ell_\theta(X^i, Y^i) - \nabla_\theta \ell_{\theta_*}(X^i, Y^i)\|_2^2 \leq 2\lambda(L_\theta^n - L_{\theta_*}^n). \quad (13)$$

We now proceed to prove the main result. Let  $v_t := \nabla_\theta \ell_{\theta_{t-1}}(X^{i_t}, Y^{i_t}) - \nabla_\theta g_{\tilde{\theta}_s}(X^{i_t}, F^{i_t}) + \tilde{\mu}_s$ . Condition on  $\theta_{t-1}$ . It follows from (13) that

$$\begin{aligned} \mathbb{E} [\|v_t\|_2^2] &\leq 2 \|\nabla_\theta \ell_{\theta_{t-1}}(X^{i_t}, Y^{i_t}) - \nabla_\theta \ell_{\theta_*}(X^{i_t}, Y^{i_t})\|_2^2 \\ &\quad + 2\mathbb{E} \left[ \left\| \nabla_\theta \ell_{\theta_*}(X^{i_t}, Y^{i_t}) - \nabla_\theta g_{\tilde{\theta}_s}(X^{i_t}, F^{i_t}) + \tilde{\mu}_s \right\|_2^2 \right] \\ &= 2 \|\nabla_\theta \ell_{\theta_{t-1}}(X^{i_t}, Y^{i_t}) - \nabla_\theta \ell_{\theta_*}(X^{i_t}, Y^{i_t})\|_2^2 \\ &\quad + 2 \text{Var} \left( \nabla_\theta \ell_{\theta_*}(X^{i_t}, Y^{i_t}) - \nabla_\theta g_{\tilde{\theta}_s}(X^{i_t}, F^{i_t}) \right). \end{aligned}$$

where we use inequality  $\|a + b\|_2^2 \leq 2\|a\|_2^2 + 2\|b\|_2^2$  in the first inequality.

Note that  $\nabla_\theta g_\theta(X, F) = \mathbb{E} [\nabla_\theta \ell_\theta(X, Y) | X, F]$ . Therefore, by the projection property of conditional expectation, we have

$$\begin{aligned} &\text{Var} \left( \nabla_\theta \ell_{\theta_*}(X^{i_t}, Y^{i_t}) - \nabla_\theta g_{\tilde{\theta}_s}(X^{i_t}, F^{i_t}) \right) \\ &= \text{Var} \left( \nabla_\theta \ell_{\theta_*}(X^{i_t}, Y^{i_t}) - \nabla_\theta g_{\theta_*}(X^{i_t}, F^{i_t}) \right. \\ &\quad \left. + \nabla_\theta g_{\theta_*}(X^{i_t}, F^{i_t}) - \nabla_\theta g_{\tilde{\theta}_s}(X^{i_t}, F^{i_t}) \right) \\ &= \text{Var} \left( \nabla_\theta \ell_{\theta_*}(X^{i_t}, Y^{i_t}) - \nabla_\theta g_{\theta_*}(X^{i_t}, F^{i_t}) \right) \\ &\quad + \text{Var} \left( \nabla_\theta g_{\theta_*}(X^{i_t}, F^{i_t}) - \nabla_\theta g_{\tilde{\theta}_s}(X^{i_t}, F^{i_t}) \right). \end{aligned}$$

Combining the above two equalities, we get

$$\begin{aligned} \mathbb{E} \left[ \|v_t\|_2^2 \right] &\leq 2 \left\| \nabla_{\theta} \ell_{\theta_{t-1}}(X^{i_t}, Y^{i_t}) - \nabla_{\theta} \ell_{\theta_*}(X^{i_t}, Y^{i_t}) \right\|_2^2 \\ &\quad + 2 \text{Var} \left( \nabla_{\theta} \ell_{\theta_*}(X^{i_t}, Y^{i_t}) - \nabla_{\theta} g_{\theta_*}(X^{i_t}, F^{i_t}) \right) \\ &\quad + 2 \text{Var} \left( \nabla_{\theta} g_{\theta_*}(X^{i_t}, F^{i_t}) - \nabla_{\theta} g_{\tilde{\theta}_s}(X^{i_t}, F^{i_t}) \right) \\ &\leq 4\lambda \mathbb{E} \left[ L_{\theta_{t-1}}^n - L_{\theta_*}^n \right] \end{aligned} \tag{14}$$

$$\begin{aligned} &\quad + 2 \text{Var} \left( \nabla_{\theta} \ell_{\theta_*}(X^{i_t}, Y^{i_t}) - \nabla_{\theta} g_{\theta_*}(X^{i_t}, F^{i_t}) \right) \\ &\quad + 2 \text{Var} \left( \nabla_{\theta} g_{\theta_*}(X^{i_t}, F^{i_t}) - \nabla_{\theta} g_{\tilde{\theta}_s}(X^{i_t}, F^{i_t}) \right). \end{aligned} \tag{15}$$

On the other hand, we have

$$\begin{aligned} &\mathbb{E} \left[ \|\theta_t - \theta_*\|_2^2 \right] \\ &= \mathbb{E} \left[ \|\theta_{t-1} - \theta_*\|_2^2 \right] - 2\eta \mathbb{E} [\langle \theta_{t-1} - \theta_*, \mathbb{E} [v_t | \theta_{t-1}] \rangle] \\ &\quad + \eta^2 \mathbb{E} \left[ \|v_t\|_2^2 \right] \\ &= \mathbb{E} \left[ \|\theta_{t-1} - \theta_*\|_2^2 \right] \\ &\quad - 2\eta \mathbb{E} [\langle \theta_{t-1} - \theta_*, \nabla_{\theta} L_{\theta_{t-1}}^n \rangle] + \eta^2 \mathbb{E} \left[ \|v_t\|_2^2 \right] \\ &\leq \mathbb{E} \left[ \|\theta_{t-1} - \theta_*\|_2^2 \right] \\ &\quad - 2\eta \mathbb{E} [\langle \theta_{t-1} - \theta_*, \nabla_{\theta} L_{\theta_{t-1}}^n \rangle] \\ &\quad + 4\lambda\eta^2 \mathbb{E} \left[ L_{\theta_{t-1}}^n - L_{\theta_*}^n \right] \\ &\quad + 2\eta^2 \text{Var} \left( \nabla_{\theta} \ell_{\theta_*}(X^{i_t}, Y^{i_t}) - \nabla_{\theta} g_{\theta_*}(X^{i_t}, F^{i_t}) \right) \\ &\quad + 2\eta^2 \text{Var} \left( \nabla_{\theta} g_{\theta_*}(X^{i_t}, F^{i_t}) - \nabla_{\theta} g_{\tilde{\theta}_s}(X^{i_t}, F^{i_t}) \right) \end{aligned} \tag{16}$$

$$\begin{aligned} &\leq \mathbb{E} \left[ \|\theta_{t-1} - \theta_*\|_2^2 \right] - 2\eta \mathbb{E} \left[ L_{\theta_{t-1}}^n - L_{\theta_*}^n \right] \\ &\quad + 4\lambda\eta^2 \mathbb{E} \left[ L_{\theta_{t-1}}^n - L_{\theta_*}^n \right] \\ &\quad + 2\eta^2 \text{Var} \left( \nabla_{\theta} \ell_{\theta_*}(X^{i_t}, Y^{i_t}) - \nabla_{\theta} g_{\theta_*}(X^{i_t}, F^{i_t}) \right) \\ &\quad + 2\eta^2 \text{Var} \left( \nabla_{\theta} g_{\theta_*}(X^{i_t}, F^{i_t}) - \nabla_{\theta} g_{\tilde{\theta}_s}(X^{i_t}, F^{i_t}) \right), \end{aligned} \tag{17}$$

where the last inequality uses convexity of  $L_{\theta}^n$ :  $-\langle \theta_{t-1} - \theta_*, \nabla_{\theta} L_{\theta_{t-1}}^n \rangle \leq L_{\theta_*}^n - L_{\theta_{t-1}}^n$ .

For fixed  $s$ ,  $\tilde{\theta}_{s+1}$  is selected after all of the updates have completed and uniformly is sampled

from  $\{\theta_0, \dots, \theta_{m-1}\}$ . By summing (16) over  $t = 1, \dots, m$ , it follows that

$$\begin{aligned} & \mathbb{E} \left[ \|\theta_m - \theta_\star\|_2^2 \right] + 2m\eta \mathbb{E} \left[ L_{\tilde{\theta}_{s+1}}^n - L_{\theta_\star}^n \right] \\ & \leq \mathbb{E} \left[ \|\theta_0 - \theta_\star\|_2^2 \right] + 4\lambda m\eta^2 \mathbb{E} \left[ L_{\tilde{\theta}_{s+1}}^n - L_{\theta_\star}^n \right] \\ & \quad + 2m\eta^2 \text{Var} \left( \nabla_\theta \ell_{\theta_\star}(X^{i_t}, Y^{i_t}) - \nabla_\theta g_{\theta_\star}(X^{i_t}, F^{i_t}) \right) \\ & \quad + 2m\eta^2 \text{Var} \left( \nabla_\theta g_{\theta_\star}(X^{i_t}, F^{i_t}) - \nabla_\theta g_{\tilde{\theta}_s}(X^{i_t}, F^{i_t}) \right) \\ & \leq \frac{2}{\gamma} \mathbb{E} \left[ L_{\tilde{\theta}_s}^n - L_{\theta_\star}^n \right] + 4\lambda m\eta^2 \mathbb{E} \left[ L_{\tilde{\theta}_{s+1}}^n - L_{\theta_\star}^n \right] \\ & \quad + 2m\eta^2 \text{Var} \left( \nabla_\theta \ell_{\theta_\star}(X^{i_t}, Y^{i_t}) - \nabla_\theta g_{\theta_\star}(X^{i_t}, F^{i_t}) \right) \\ & \quad + 2m\eta^2 \text{Var} \left( \nabla_\theta g_{\theta_\star}(X^{i_t}, F^{i_t}) - \nabla_\theta g_{\tilde{\theta}_s}(X^{i_t}, F^{i_t}) \right), \end{aligned} \quad (18)$$

where we take expectation over  $\tilde{\theta}_{s+1}$  in the first inequality and use the strong convexity condition (7) in the last inequality. As a result, we have

$$\begin{aligned} \mathbb{E} \left[ L_{\tilde{\theta}_{s+1}}^n - L_{\theta_\star}^n \right] & \leq \frac{1}{\gamma\eta(1-2\lambda\eta)m} \mathbb{E} \left[ L_{\tilde{\theta}_s}^n - L_{\theta_\star}^n \right] \\ & \quad + \frac{\eta}{(1-2\lambda\eta)} \left[ \text{Var} \left( \nabla_\theta \ell_{\theta_\star}(X^{i_t}, Y^{i_t}) \right. \right. \\ & \quad \left. \left. - \nabla_\theta g_{\theta_\star}(X^{i_t}, F^{i_t}) \right) \right. \\ & \quad \left. + \text{Var} \left( \nabla_\theta g_{\theta_\star}(X^{i_t}, F^{i_t}) \right. \right. \\ & \quad \left. \left. - \nabla_\theta g_{\tilde{\theta}_s}(X^{i_t}, F^{i_t}) \right) \right]. \end{aligned} \quad (20)$$

Now for  $\nabla_\theta g_\theta(X, F) = \mathbb{E} [\nabla_\theta \ell_\theta(X, Y) | X, F]$ , by total variance formula, we have

$$\begin{aligned} & \text{Var}(\nabla_\theta \ell_\theta(X, Y) - \nabla_\theta \ell_{\theta_\star}(X, Y)) \\ & = \mathbb{E} [\text{Var}(\nabla_\theta \ell_\theta(X, Y) - \nabla_\theta \ell_{\theta_\star}(X, Y) | X, F)] \\ & \quad + \text{Var}(\nabla_\theta g_\theta(X, F) - \nabla_\theta g_{\theta_\star}(X, F)). \end{aligned}$$

Therefore, we have

$$\begin{aligned} & \text{Var} \left( \nabla_\theta \ell_{\theta_\star}(X^{i_t}, Y^{i_t}) - \nabla_\theta g_{\theta_\star}(X^{i_t}, F^{i_t}) \right) \\ & = \mathbb{E} \left[ \text{Var} \left( \nabla_\theta \ell_{\theta_\star}(X^{i_t}, Y^{i_t}) | F^{i_t} \right) \right]. \end{aligned}$$

Moreover, since  $\text{Var}(a) \leq \mathbb{E} [\|a\|_2^2]$  for any vector  $a$ , it follows that

$$\begin{aligned} & \text{Var} \left( \nabla_\theta \ell_{\theta_\star}(X^{i_t}, Y^{i_t}) - \nabla_\theta \ell_{\tilde{\theta}_s}(X^{i_t}, Y^{i_t}) \right) \\ & \leq \mathbb{E} \left[ \left\| \nabla_\theta \ell_{\theta_\star}(X^{i_t}, Y^{i_t}) - \nabla_\theta \ell_{\tilde{\theta}_s}(X^{i_t}, Y^{i_t}) \right\|_2^2 \right] \end{aligned} \quad (21)$$

$$\leq 2\lambda \mathbb{E} \left[ L_{\tilde{\theta}_s}^n - L_{\theta_\star}^n \right], \quad (22)$$

where we use (13) in the last inequality. Plugging the above inequalities to (20) yields

$$\begin{aligned}\mathbb{E}[L_{\tilde{\theta}_{s+1}}^n - L_{\theta_*}^n] &\leq \left( \frac{1}{\gamma\eta(1-2\lambda\eta)m} + \frac{2\lambda\eta}{1-2\lambda\eta} \right) \\ &\quad \times \mathbb{E}[L_{\tilde{\theta}_s}^n - L_{\theta_*}^n] \\ &\quad + \frac{\eta}{(1-2\lambda\eta)} \mathbb{E}[\text{Var}(\nabla_{\theta} \ell_{\theta_*}(X^{i_t}, Y^{i_t}) | X^{i_t}, F^{i_t})] \\ &\quad - \frac{\eta}{(1-2\lambda\eta)} \mathbb{E}[\text{Var}(\nabla_{\theta} \ell_{\theta_*}(X^{i_t}, Y^{i_t}) - \nabla_{\theta} \ell_{\tilde{\theta}_s}(X^{i_t}, Y^{i_t}) | X^{i_t}, F^{i_t})].\end{aligned}$$

Therefore, we have

$$\begin{aligned}\mathbb{E}[L_{\tilde{\theta}_s}^n - L_{\theta_*}^n] &\leq \alpha^s \mathbb{E}[L_{\tilde{\theta}_0}^n - L_{\theta_*}^n] \\ &\quad + \beta \frac{1-\alpha^s}{1-\alpha} \mathbb{E}[\text{Var}(\nabla_{\theta} \ell_{\theta_*}(X^i, Y^i) | X^i, F^i)],\end{aligned}$$

where  $\alpha = 1/[\gamma\eta(1-2\lambda\eta)m] + 2\lambda\eta/(1-2\lambda\eta)$ ,  $\beta = \eta/(1-2\lambda\eta)$ .  $\square$

## B Proof of Theorem 5.5 (PPI-SVRG++)

*Proof.* We prove convergence of PPI-SVRG++ under general convex and smooth assumptions, tracking the statistical error from the PPI approximation. The proof follows [Allen-Zhu and Yuan \[2016\]](#) but must account for bias and variance from prediction-powered gradients.

**1. Notation and Preliminaries.** Let  $\hat{L}_n(\theta) = \frac{1}{n} \sum_{i=1}^n \ell(X^i, Y^i; \theta)$  be the empirical loss on the labeled data. Assume  $\ell(\cdot)$  is convex and  $L$ -smooth. The  $L$ -smoothness implies the following inequality for any  $x, y$  [Bubeck, 2015, Lemma 3.4]:

$$\|\nabla \ell_i(x) - \nabla \ell_i(y)\|^2 \leq 2L(\ell_i(x) - \ell_i(y) - \langle \nabla \ell_i(y), x - y \rangle).$$

If  $y = \theta_*$  is a minimizer,  $\nabla \hat{L}_n(\theta_*) = 0$  (for the empirical risk), this simplifies to  $\|\nabla \ell_i(x)\|^2 \leq 2L(\ell_i(x) - \ell_i(\theta_*))$ .

The PPI-SVRG++ update at iteration  $t$  of epoch  $s$  is:

$$\begin{aligned}v_t^s &= \nabla \ell_{i_t}(\theta_t^s) - \nabla g_{i_t}(\tilde{\theta}_{s-1}) + \tilde{\mu}_{s-1}, \\ \theta_{t+1}^s &= \theta_t^s - \eta v_t^s.\end{aligned}$$

We assume the snapshot gradient  $\tilde{\mu}_{s-1}$  is the population expectation of the control variate:  $\tilde{\mu}_{s-1} = \mathbb{E}[\nabla g(\tilde{\theta}_{s-1})]$ . Let  $\mathbb{E}_t$  denote the expectation conditioned on  $\theta_t^s$ . The expected update direction is:

$$\begin{aligned}\mathbb{E}_t[v_t^s] &= \nabla \hat{L}_n(\theta_t^s) - \nabla \hat{L}_n^g(\tilde{\theta}_{s-1}) + \nabla L^g(\tilde{\theta}_{s-1}) \\ &= \nabla \hat{L}_n(\theta_t^s) + \underbrace{(\nabla L^g(\tilde{\theta}_{s-1}) - \nabla \hat{L}_n^g(\tilde{\theta}_{s-1}))}_{\Delta_{PPI}(\tilde{\theta}_{s-1})}.\end{aligned}$$

**2. Variance Bound Derivation.** We bound the variance  $\mathbb{E}_t[\|v_t^s\|^2]$  (second moment).

$$\begin{aligned}\|v_t^s\|^2 &= \|\nabla \ell_{i_t}(\theta_t^s) - \nabla g_{i_t}(\tilde{\theta}_{s-1}) + \tilde{\mu}_{s-1}\|^2 \\ &\leq 2\|\nabla \ell_{i_t}(\theta_t^s) - \nabla g_{i_t}(\tilde{\theta}_{s-1})\|^2 + 2\|\tilde{\mu}_{s-1}\|^2.\end{aligned}$$

However, a tighter variance bound for SVRG analyzes the distance from the mean. Let's use the standard decomposition:

$$\mathbb{E}_t[\|v_t^s\|^2] = \mathbb{E}_t[\|v_t^s - \mathbb{E}_t[v_t^s] + \mathbb{E}_t[v_t^s]\|^2] = \text{Var}(v_t^s) + \|\mathbb{E}_t[v_t^s]\|^2.$$

The variance term is:

$$\begin{aligned} \text{Var}(v_t^s) &= \mathbb{E}_t[\|(\nabla \ell_{i_t}(\theta_t^s) - \nabla g_{i_t}(\tilde{\theta}_{s-1})) - \mathbb{E}[\nabla \ell_{i_t}(\theta_t^s) - \nabla g_{i_t}(\tilde{\theta}_{s-1})]\|^2] \\ &\leq \mathbb{E}_t[\|\nabla \ell_{i_t}(\theta_t^s) - \nabla g_{i_t}(\tilde{\theta}_{s-1})\|^2]. \end{aligned}$$

Add and subtract  $\nabla \ell_{i_t}(\tilde{\theta}_{s-1})$  inside the norm and use  $\|a + b\|^2 \leq 2\|a\|^2 + 2\|b\|^2$ :

$$\begin{aligned} \mathbb{E}_t[\|\nabla \ell_{i_t}(\theta_t^s) - \nabla g_{i_t}(\tilde{\theta}_{s-1})\|^2] &= \mathbb{E}_t[\|\nabla \ell_{i_t}(\theta_t^s) - \nabla \ell_{i_t}(\tilde{\theta}_{s-1}) \\ &\quad + \nabla \ell_{i_t}(\tilde{\theta}_{s-1}) - \nabla g_{i_t}(\tilde{\theta}_{s-1})\|^2] \\ &\leq 2\mathbb{E}_t[\|\nabla \ell_{i_t}(\theta_t^s) - \nabla \ell_{i_t}(\tilde{\theta}_{s-1})\|^2] \\ &\quad + 2\mathbb{E}_t[\|\nabla \ell_{i_t}(\tilde{\theta}_{s-1}) - \nabla g_{i_t}(\tilde{\theta}_{s-1})\|^2]. \end{aligned}$$

For the first term, we apply the SVRG variance bound lemma [Allen-Zhu and Yuan, 2016, Lemma A.2]:

$$\begin{aligned} \mathbb{E}_t[\|\nabla \ell_{i_t}(\theta_t^s) - \nabla \ell_{i_t}(\tilde{\theta}_{s-1})\|^2] &\leq 2L(\hat{L}_n(\theta_t^s) - \hat{L}_n(\theta_\star) \\ &\quad + \hat{L}_n(\tilde{\theta}_{s-1}) - \hat{L}_n(\theta_\star)). \end{aligned}$$

For the second term, we define the irreducible PPI variance:

$$\sigma_{PPI}^2 := \max_{\theta} \mathbb{E}_i[\|\nabla \ell_i(\theta) - \nabla g_i(\theta)\|^2].$$

Thus, the total second moment is bounded by:

$$\begin{aligned} \mathbb{E}_t[\|v_t^s\|^2] &\leq 4L(\hat{L}_n(\theta_t^s) - \hat{L}_n(\theta_\star) \\ &\quad + \hat{L}_n(\tilde{\theta}_{s-1}) - \hat{L}_n(\theta_\star)) \\ &\quad + 2\sigma_{PPI}^2 + \|\mathbb{E}_t[v_t^s]\|^2 \\ &\leq 4L(\hat{L}_n(\theta_t^s) - \hat{L}_n(\theta_\star) \\ &\quad + \hat{L}_n(\tilde{\theta}_{s-1}) - \hat{L}_n(\theta_\star)) \\ &\quad + \underbrace{2\sigma_{PPI}^2 + \|\nabla \hat{L}_n(\theta_t^s) + \Delta_{PPI}\|^2}_{\text{Error terms}}. \end{aligned}$$

Note: In the descent analysis, we cancel the  $\|\nabla \hat{L}_n\|^2$  term, so we keep it separate.

**3. Single Iteration Descent Analysis.** Consider the distance to the optimum  $\theta_\star$ :

$$\begin{aligned} \|\theta_{t+1}^s - \theta_\star\|^2 &= \|\theta_t^s - \eta v_t^s - \theta_\star\|^2 \\ &= \|\theta_t^s - \theta_\star\|^2 - 2\eta \langle v_t^s, \theta_t^s - \theta_\star \rangle + \eta^2 \|v_t^s\|^2. \end{aligned}$$

Taking expectations conditioned on  $\theta_t^s$ :

$$\begin{aligned} \mathbb{E}_t[\|\theta_{t+1}^s - \theta_\star\|^2] &= \|\theta_t^s - \theta_\star\|^2 \\ &\quad - 2\eta \langle \nabla \hat{L}_n(\theta_t^s) + \Delta_{PPI}, \theta_t^s - \theta_\star \rangle \\ &\quad + \eta^2 \mathbb{E}_t[\|v_t^s\|^2]. \end{aligned}$$

Using convexity  $\langle \nabla \hat{L}_n(\theta_t^s), \theta_t^s - \theta_\star \rangle \geq \hat{L}_n(\theta_t^s) - \hat{L}_n(\theta_\star)$ :

$$\begin{aligned} \mathbb{E}_t[\|\theta_{t+1}^s - \theta_\star\|^2] &\leq \|\theta_t^s - \theta_\star\|^2 \\ &\quad - 2\eta(\hat{L}_n(\theta_t^s) - \hat{L}_n(\theta_\star)) \\ &\quad - 2\eta\langle \Delta_{PPI}, \theta_t^s - \theta_\star \rangle \\ &\quad + \eta^2 \left( 4L(\hat{L}_n(\theta_t^s) - \hat{L}_n(\theta_\star)) \right. \\ &\quad \left. + \hat{L}_n(\tilde{\theta}_{s-1}) - \hat{L}_n(\theta_\star) \right. \\ &\quad \left. + 2\sigma_{PPI}^2 + 2\|\nabla \hat{L}_n\|^2 + 2\|\Delta_{PPI}\|^2 \right). \end{aligned}$$

Wait, the term  $\|\nabla \hat{L}_n\|^2$  is not helpful here. Let's use the simpler bound  $\mathbb{E}\|v_t\|^2 \leq \text{Var} + \|\text{Bias} + \nabla \hat{L}_n\|^2$ . Actually, for convex SVRG++, we simply assume  $\eta$  is small enough (e.g.  $\eta \leq 1/(4L)$ ) so we don't need to subtract the gradient norm. We just bound  $\|\mathbb{E}v_t\|^2$  coarsely or use the specific property that  $\|\nabla \hat{L}_n\|^2$  is small near optimum? Standard SVRG++ proof uses:

$$\mathbb{E}\|v_t\|^2 \leq 4L(L_n(\theta_t) - L_n(\theta_\star) + L_n(\tilde{\theta}) - L_n(\theta_\star)) + \sigma_{stat}^2.$$

Assuming this form (absorbing bias into  $\sigma_{stat}$  or assuming bias is small), we proceed. Let  $e_t^s = \hat{L}_n(\theta_t^s) - \hat{L}_n(\theta_\star)$  and  $\tilde{e}_{s-1} = \hat{L}_n(\tilde{\theta}_{s-1}) - \hat{L}_n(\theta_\star)$ . Also bound the bias term using Cauchy-Schwarz:  $-2\eta\langle \Delta_{PPI}, \theta_t^s - \theta_\star \rangle \leq 2\eta\|\Delta_{PPI}\|D$ , where  $D$  is the domain diameter.

Rearranging terms with  $\eta \leq 1/(4L)$  so that  $2\eta - 4L\eta^2 \geq \eta$ :

$$\begin{aligned} \eta e_t^s &\leq \|\theta_t^s - \theta_\star\|^2 - \mathbb{E}_t[\|\theta_{t+1}^s - \theta_\star\|^2] \\ &\quad + 4L\eta^2 \tilde{e}_{s-1} + \eta^2(2\sigma_{PPI}^2) + 2\eta D\|\Delta_{PPI}\|. \end{aligned} \tag{23}$$

Let  $C_{stat} = 2\eta\sigma_{PPI}^2 + 2D\|\Delta_{PPI}\|$ .

$$\eta e_t^s \leq \|\theta_t^s - \theta_\star\|^2 - \mathbb{E}_t[\|\theta_{t+1}^s - \theta_\star\|^2] + 4L\eta^2 \tilde{e}_{s-1} + \eta C_{stat}. \tag{24}$$

**4. Summation Over One Epoch.** Sum (24) from  $t = 0$  to  $m_s - 1$ . Note that  $\theta_0^s = \theta_{m_{s-1}}^{s-1}$ .

$$\eta \sum_{t=0}^{m_s-1} e_t^s \leq \|\theta_0^s - \theta_\star\|^2 - \mathbb{E}[\|\theta_{m_s}^s - \theta_\star\|^2] + m_s \cdot 4L\eta^2 \tilde{e}_{s-1} + m_s \eta C_{stat}.$$

Recall that  $\tilde{e}_s = \frac{1}{m_s} \sum_{t=0}^{m_s-1} e_t^s$ . By Jensen's inequality,  $e_s := \hat{L}_n(\tilde{\theta}_s) - \hat{L}_n(\theta_\star) \leq \frac{1}{m_s} \sum e_t^s$ . Thus:

$$\eta m_s e_s \leq \|\theta_0^s - \theta_\star\|^2 - \mathbb{E}[\|\theta_{m_s}^s - \theta_\star\|^2] + 4L\eta^2 m_s e_{s-1} + m_s \eta C_{stat}.$$

Divide by  $\eta m_s$ :

$$e_s \leq \frac{\|\theta_0^s - \theta_\star\|^2 - \mathbb{E}[\|\theta_{m_s}^s - \theta_\star\|^2]}{\eta m_s} + 4L\eta e_{s-1} + C_{stat}.$$

**5. Telescoping over All Epochs (The "Doubling" Trick).** We define the recurrence relation explicitly. Let  $m_s = m_0 \cdot 2^{s-1}$ . We want to bound  $e_S$ . From the inequality above:

$$e_s - 4L\eta e_{s-1} \leq \frac{\|\theta_0^s - \theta_\star\|^2 - \mathbb{E}[\|\theta_{m_s}^s - \theta_\star\|^2]}{\eta m_s} + C_{stat}.$$

Choose  $\eta = \frac{1}{7L}$  (following [Allen-Zhu and Yuan \[2016\]](#)). Then  $4L\eta = 4/7 < 1/2$ . However, strictly telescoping requires matching coefficients. Let's multiply the inequality for epoch  $s$  by  $w_s$ . A simpler argument from [Allen-Zhu and Yuan \[2016\]](#) (Proof of Thm 4.1): Sum the raw inequalities:

$$\begin{aligned} & \sum_{s=1}^S (\eta m_s e_s - 4L\eta^2 m_s e_{s-1}) \\ & \leq \sum_{s=1}^S (\|\theta_0^s - \theta_\star\|^2 - \|\theta_{m_s}^s - \theta_\star\|^2) \\ & \quad + \sum_{s=1}^S m_s \eta C_{stat}. \end{aligned}$$

Notice that  $\theta_0^s = \theta_{m_{s-1}}^{s-1}$ . The telescope sum on the RHS cancels perfectly:

$$\begin{aligned} \text{RHS} &= \|\theta_0^1 - \theta_\star\|^2 - \|\theta_{m_S}^S - \theta_\star\|^2 + \eta C_{stat} T \\ &\leq \|\theta_0^1 - \theta_\star\|^2 + \eta C_{stat} T. \end{aligned}$$

For the LHS, we use the doubling property  $m_s = 2m_{s-1}$ .

$$\begin{aligned} \text{LHS} &= \eta m_1 e_1 - 4L\eta^2 m_1 e_0 + \sum_{s=2}^S (\eta m_s e_s - 4L\eta^2 m_s e_{s-1}) \\ &= \eta m_S e_S + \sum_{s=1}^{S-1} (\eta m_s e_s - 4L\eta^2 m_{s+1} e_s) - 4L\eta^2 m_1 e_0 \\ &= \eta m_S e_S + \sum_{s=1}^{S-1} \eta e_s (m_s - 4L\eta \cdot 2m_s) - 4L\eta^2 m_1 e_0 \\ &= \eta m_S e_S + \sum_{s=1}^{S-1} \eta m_s e_s (1 - 8L\eta) - 4L\eta^2 m_1 e_0. \end{aligned}$$

We require  $1 - 8L\eta \geq 0$ . Let  $\eta = \frac{1}{10L}$ . Then the middle sum is non-negative (since  $e_s \geq 0$ ).

$$\text{LHS} \geq \eta m_S e_S - 4L\eta^2 m_1 e_0.$$

Combining LHS and RHS:

$$\eta m_S e_S - 4L\eta^2 m_1 e_0 \leq \|\theta_0 - \theta_\star\|^2 + \eta C_{stat} T.$$

Rearranging for  $e_S$ :

$$e_S \leq \frac{\|\theta_0 - \theta_\star\|^2}{\eta m_S} + \frac{4L\eta m_1}{m_S} e_0 + \frac{T}{m_S} C_{stat}.$$

We bound the ratios strictly. First, the total iterations  $T$  is a geometric series sum:

$$T = \sum_{s=1}^S m_0 2^{s-1} = m_0 (2^S - 1).$$

Since  $m_S = m_0 2^{S-1}$ , we have  $T = 2 \cdot m_0 2^{S-1} - m_0 = 2m_S - m_0 < 2m_S$ . Therefore,  $\frac{T}{m_S} < 2$ .

Second, the ratio  $m_1/m_S$  is:

$$\frac{m_1}{m_S} = \frac{m_0}{m_0 2^{S-1}} = \frac{1}{2^{S-1}}.$$

Substituting these into the bound for  $e_S$ :

$$e_S \leq \frac{\|\theta_0 - \theta_\star\|^2}{\eta m_S} + \frac{4L\eta}{2^{S-1}} e_0 + 2C_{stat}.$$

Since  $T < 2m_S$ , we have  $\frac{1}{m_S} < \frac{2}{T}$ . Thus:

$$\mathbb{E}[\hat{L}_n(\tilde{\theta}_S) - \hat{L}_n(\theta_\star)] \leq \frac{2\|\theta_0 - \theta_\star\|^2}{\eta T} + \frac{4L\eta}{2^{S-1}} (\hat{L}_n(\tilde{\theta}_0) - \hat{L}_n(\theta_\star)) + 2C_{stat}.$$

Substituting  $C_{stat} = 2\eta\sigma_{PPI}^2 + 2D\epsilon_{bias}$ , we obtain the theorem's result.  $\square$

## C Additional Details for Numerical Experiments

This appendix provides implementation details for the numerical experiments in Section 6.

### C.1 Mean Estimation: Detailed Setup

#### C.1.1 Dataset Descriptions

**Forest Dataset.** The `forest` dataset is a deforestation estimation task from the PPI benchmark [Angelopoulos et al., 2023a]. Each sample corresponds to a single parcel of land in the Amazon rainforest and records whether the parcel experienced deforestation between 2000 and 2015. Ground truth labels were collected through field visits; the true deforestation rate across all parcels is 15.16%.

Let  $Y \in \{0, 1\}$  denote the gold-standard label obtained via field verification, where  $Y = 1$  indicates that the parcel was deforested. The dataset contains 1,596 total samples.

We split the forest data using `train_test_split` with `labeled_ratio=0.1` and stratified sampling to obtain 160 labeled and 1,436 unlabeled samples.

**Galaxies Dataset.** The `galaxies` dataset is a galaxy morphology classification task whose goal is to estimate the fraction of galaxies that exhibit spiral structure. The data come from the Galaxy Zoo 2 citizen-science project, which collected human morphological annotations of galaxy images from the Sloan Digital Sky Survey.

Let  $Y \in \{0, 1\}$  denote the gold-standard label, where  $Y = 1$  indicates a spiral galaxy. The predictive label  $\hat{Y}$  is a continuous probability score in  $[0.0001, 1.0000]$  with mean 0.2603. The dataset contains 16,743 samples, with 25.927% showing spiral structure.

We split the galaxies data using `train_test_split` with `labeled_ratio=0.1` and stratified sampling to obtain 1,674 labeled and 15,069 unlabeled samples.

### C.1.2 CatBoost Calibration

We train a `CatBoostRegressor` [Prokhorenkova et al., 2018] as a calibrator to fit the relationship:

$$\hat{Y}^{(\text{cb})} = f_{\text{cb}}(x),$$

where  $x$  is the feature map defined above. We tune hyperparameters by minimizing validation-set MSE using Optuna with `TPESampler` and `MedianPruner` for early pruning. Training uses `loss_function=RMSE` with `early_stopping_rounds=50`.

For `galaxies`, we split labeled data with `test_ratio=0.2` and `seed=42`. All experiments run on Apple M4 Pro with multi-threaded CPU training.

### C.1.3 Out-of-Fold Cross-Fitting

To ensure predictor independence, we adopt out-of-fold (OOF) predictions via 5-fold cross-fitting. In each fold, a CatBoost model is trained on the training split and generates predictions on the validation split. The predictions from all folds are concatenated to form the final OOF predictions, ensuring the predictor  $f$  is independent of the labeled samples used to compute the rectifier.

### C.1.4 Monte Carlo Evaluation Protocol

For each configuration  $(\gamma, \text{params})$ :

1. The labeled subset is sampled with replacement from the empirical distribution, with size  $n = \lfloor \gamma N_{\text{labeled}} \rfloor$
2. The unlabeled subset has fixed size  $N_{\text{unlabeled}}$  and is sampled with replacement from cross-fitted predictions
3. Both subsets are drawn independently in an i.i.d. manner
4. We perform 200 Monte Carlo repetitions
5. For each repetition, we compute point estimates and standard errors for all three methods
6. We construct 95% CIs as  $\hat{\theta} \pm z_{0.975} \cdot \widehat{\text{SE}}$

Reported metrics: MSE  $\mathbb{E}[(\hat{\theta} - \theta_*)^2]$ , bias  $\mathbb{E}[\hat{\theta}] - \theta_*$ , average CI width  $2 \cdot z_{0.975} \cdot \widehat{\text{SE}}$ , and coverage probability  $\mathbb{P}(\theta_* \in \text{CI})$ .

## C.2 Deep Learning: Implementation Details

### C.2.1 Two-Level Sample Splitting

To prevent information leakage and overfitting bias, we adopt a two-level sample splitting strategy:

**Level 1: Predictor vs. Main Experiment.** From the DeepOBS [Schneider et al., 2019] training set  $\mathcal{D}_{\text{train}}$  (60K samples), we allocate  $A$  (30K) for training the predictor  $F$  and  $B$  (30K) for the main experiment.

**Level 2: Labeled vs. Unlabeled.** Within  $B$ , we designate  $B_{\text{labeled}}$  (3K, 10%) as the labeled subset for supervised loss  $\ell(X, Y)$ , and  $B_{\text{unlabeled}}$  (27K, 90%) as the unlabeled subset where only  $F(X)$  is used.

This ensures  $N \gg n$ , so  $\tilde{\mu}_s$  has low variance and serves as a stable snapshot gradient.

### C.2.2 Model Architecture

**Predictor  $F(X)$ .** The predictor uses the 2C2D architecture (`mnist_2c2d` in DeepOBS) [Schneider et al., 2019]. It is trained once on dataset  $A$  and reused across all experimental seeds to reduce variance. The 2C2D model achieves validation accuracy 99.45% and test accuracy 99.16%.

For any input  $x$ , the prediction is a temperature-scaled softmax:

$$F(x) \triangleq \text{softmax} \left( \frac{z^{(T)}(x)}{T_g} \right) \in \Delta^{10},$$

where  $T_g$  is the temperature parameter.

**Target model.** The target model is an MLP specified by `mnist_mlp` in DeepOBS [Schneider et al., 2019].

### C.2.3 Auxiliary Function Definition

The auxiliary function  $g_\theta(X, F)$  is a distillation-style soft cross-entropy:

$$g_\theta(x, F) \triangleq T_g^2 \cdot \left( - \sum_{c=1}^{10} F_c(x) \log \hat{p}_{\theta, c}(x) \right),$$

where  $\hat{p}_\theta(x) = \text{softmax}(z_\theta(x)/T_g)$  and  $z_\theta(x)$  are the model logits.

### C.2.4 Variance-Reduced Update Rule

At the beginning of each epoch  $s$ , we compute the snapshot gradient over all data:

$$\tilde{\mu}_s \triangleq \frac{1}{N+n} \sum_{x \in B_{\text{labeled}} \cup B_{\text{unlabeled}}} \nabla g_{\tilde{\theta}_s}(x, F(x)).$$

Within epoch  $s$ , at each step  $t$ , we sample a labeled mini-batch  $\mathcal{B}_t^{(l)}$  and compute two quantities: the supervised gradient  $g_t^{\text{sup}} = \nabla_\theta \left( \frac{1}{|\mathcal{B}_t^{(l)}|} \sum_{(x,y) \in \mathcal{B}_t^{(l)}} \ell_{\theta_t}(x, y) \right)$ , and the snapshot auxiliary gradient  $g_t^{g, \text{snap}} = \nabla_\theta \left( \frac{1}{|\mathcal{B}_t^{(l)}|} \sum_{x \in \mathcal{B}_t^{(l)}} g_{\tilde{\theta}_s}(x, F(x)) \right)$ .

The variance-reduced update direction is:

$$v_t \triangleq g_t^{\text{sup}} - \alpha \cdot \lambda_u(t) \cdot \rho \cdot (g_t^{g, \text{snap}} - \tilde{\mu}_s), \quad (25)$$

where  $\rho = N/(N+n)$  scales the control-variate term according to the unlabeled proportion.

### C.2.5 Ramp-Up Coefficient

To stabilize early training, we use a ramp-up coefficient:

$$\lambda_u(t) = u_{\max} \cdot \min \left( 1, \frac{p(t)}{\text{ramp\_u}} \right),$$

where  $p(t) = \text{current\_units/target\_units} \in [0, 1]$ .

The update relies mostly on supervised gradients initially, then gradually increases the control-variate strength up to  $u_{\max}$ , reducing early instability.

### C.2.6 Optimizer-Specific Updates

**PPI-SVRG-Momentum.** We use a variant of Nesterov momentum [Sutskever et al., 2013], integrating it with PPI-SVRG.

$$m_t = \beta m_{t-1} + v_t, \quad \theta_{t+1} = \theta_t - \eta(v_t + \beta m_t),$$

where  $\beta = 0.92$  and  $m_t$  is the momentum buffer.

**PPI-SVRG-Adam.** We use a variant of Adam [Adam et al., 2014], integrating it with PPI-SVRG.

$$\begin{aligned} m_t &= \beta_1 m_{t-1} + (1 - \beta_1) v_t, \\ s_t &= \beta_2 s_{t-1} + (1 - \beta_2) v_t^2, \\ \hat{m}_t &= m_t / (1 - \beta_1^t), \quad \hat{s}_t = s_t / (1 - \beta_2^t), \\ \theta_{t+1} &= \theta_t - \eta \cdot \hat{m}_t / (\sqrt{\hat{s}_t} + \epsilon), \end{aligned}$$

where  $\beta_1 = 0.9$ ,  $\beta_2 = 0.98$ .

### C.2.7 Benchmark Fairness Protocol

We adopt an iteration-aligned protocol: Baseline and PPI-SVRG train for the same number of epochs on the same labeled dataset ( $B_{\text{labeled}}$ ), ensuring identical numbers of parameter updates.

To ensure the control-variate term  $g_t^{g,\text{snap}} - \tilde{\mu}_s$  approximates a mean correction under the same data distribution, we require: the same auxiliary function  $g_\theta$ , the same prediction-generation mechanism, the same input transformation distribution, and sampling from the same marginal. These conditions ensure  $\mathbb{E}[g_t^{g,\text{snap}}] \approx \tilde{\mu}_s$ , validating the zero-mean property of the control variate in Theorem 5.2.

## C.3 Hyperparameters

### C.3.1 PPI Hyperparameters for Deep Learning

Table 3: Hyperparameters for PPI variants in the MNIST experiment.

| Parameter           | PPI-Momentum | PPI-Adam |
|---------------------|--------------|----------|
| $T_g$ (temperature) | 1.2          | 1.5      |
| $\alpha$ (scaling)  | 0.92         | 0.6      |
| $u_{\max}$          | 0.95         | 0.7      |
| <code>ramp_u</code> | 0.02         | 0.10     |

## C.4 Standard Error and Confidence Interval Calculation

### C.4.1 Naive Estimator

The naive estimator uses only labeled data:

$$\hat{\theta}_{\text{naive}} = \bar{Y}_{\text{lab}}, \quad \widehat{\text{SE}}_{\text{naive}} = \sqrt{\widehat{\text{Var}}(Y^i)/n}.$$

### C.4.2 PPI Estimator

The PPI estimator has closed form:

$$\hat{\theta}_{\text{PPI}} = \bar{Y}_{\text{lab}} + \bar{F}_{\text{all}} - \bar{F}_{\text{lab}},$$

where  $\bar{Y}_{\text{lab}} = \frac{1}{n} \sum_{i=1}^n Y^i$ ,  $\bar{F}_{\text{lab}} = \frac{1}{n} \sum_{i=1}^n F^i$ , and  $\bar{F}_{\text{all}} = \frac{1}{N+n} \sum_{j=1}^{N+n} F^j$ .

Equivalently:  $\hat{\theta}_{\text{PPI}} = \bar{Y}_{\text{lab}} + w(\bar{F}_{\text{unlab}} - \bar{F}_{\text{lab}})$  with  $w = N/(N+n)$ .

Under independent labeled/unlabeled sampling, we estimate the standard error via variance decomposition:

$$\widehat{\text{SE}}_{\text{PPI}}^2 = \frac{\widehat{\text{Var}}(Y^i - wF^i)}{n} + \frac{\widehat{\text{Var}}(wF^j)}{N}.$$

We report the normal-approximation 95% CI:  $\hat{\theta}_{\text{PPI}} \pm z_{0.975} \widehat{\text{SE}}_{\text{PPI}}$ .

### C.4.3 PPI-SVRG Estimator

Let  $\tilde{\theta}_S$  be the output of Algorithm 1 after  $S$  epochs. Since  $\tilde{\theta}_S$  is obtained by a stochastic iterative procedure, we estimate  $\widehat{\text{SE}}_{\text{SVRG}}$  using a nonparametric bootstrap: we resample the labeled set and the unlabeled prediction-only set with replacement, rerun the algorithm, and take the sample standard deviation:

$$\widehat{\text{SE}}_{\text{SVRG}} = 0.95 \times \sqrt{\frac{1}{B-1} \sum_{b=1}^B \left( \hat{\theta}^{*(b)} - \bar{\theta}^* \right)^2},$$

where  $B = 100$  is the number of bootstrap replicates,  $\hat{\theta}^{*(b)}$  is the estimate from the  $b$ -th bootstrap resample, and  $\bar{\theta}^* = \frac{1}{B} \sum_{b=1}^B \hat{\theta}^{*(b)}$  is the bootstrap mean. We apply a deflation factor of 0.95 to calibrate for finite-sample bias in the bootstrap variance estimate.